ORIGINAL PAPERS

Spectra and photorelaxation of tris-biphenyl-triazine-type UV absorbers: from monomers to nanoparticles

Sergej Naumov[1] · Bernd Herzog[2] · Bernd Abel[1,3]

Abstract

Water-insoluble organic UV filters like tris-biphenyl-triazine (TBPT) can be prepared as aqueous dispersions of nanoparticles. The particles consist of the respective UV absorber molecules and show strong UV absorbance. Since there is a certain solubility of such UV absorbers in organic solvents, it is possible to measure the absorbance spectrum also in solution, for instance in ethanol or dioxane. The UV spectrum of the aqueous dispersion shows a slight hypsochromic shift of the original band with an additional shoulder at longer wavelengths. For the understanding of the observed changes of UV–Vis spectra of this UV absorber, either dissolved in an organic solvent or dispersed as nanoparticles in water, DFT calculations were carried out with the respective monomer and aggregates of TBPT molecules in the different media. The calculated UV–Vis spectra of isolated, that means dissolved, TBPT molecules in ethanol and in dioxane agree well with experimentally observed ones. The observed changes in the shape of experimental UV–Vis spectra in aqueous dispersion cannot be explained with a solvent effect only. It was found that the studied molecules could form stable energetically favorable π-stacked aggregates, which show UV–Vis spectra in reasonable agreement with those experimentally observed in aqueous dispersion. Such aggregates of TBPT are most likely the reason for the observed additional shoulder in the UV/vis absorbance spectrum. In addition, the mechanism of the photochemical deactivation of excited TBPT molecules was studied in detail with TD DFT in dioxane and in water.

Graphical abstract
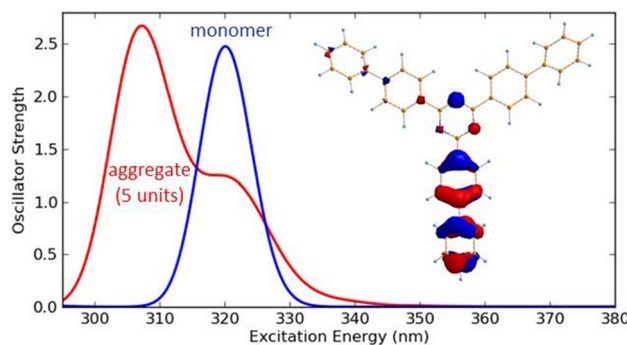
1 Introduction

Sunscreens used for the protection of human skin against the harmful effects of solar radiation contain high concentrations of UV-absorbing molecules [1, 2]. For the use

---

Extended author information available on the last page of the article

in sunscreens, such UV filters must be approved by the responsible authorities after toxicological assessment. Approval always implies a maximum concentration, up to which the respective UV filter can be incorporated in a sunscreen preparation. Most of such substances are oil-soluble, if solid at ambient conditions, or even oil-miscible, if liquid at ambient conditions, and consequently are incorporated into the oil phase of sunscreen preparations. The maximum concentration at which a UV absorber can be incorporated in the oil phase is often limited by its solubility. To circumvent this difficulty, UV absorbers showing very poor solubility in oils as well as in water have been prepared as nano-particulate aqueous dispersions by wet-milling procedures, with median diameters of the particles in the range between 100 and 160 nm, based on volume-weighted particle size distributions [3, 4]. In this way, it is possible to load substantial amounts of UV-absorbing material into the water-phase of sunscreen preparations. This has been demonstrated with a hydroxyphenyl-benzotriazole-type UV absorber and also with a tris-biphenyl-triazine-type UV absorber. It has been shown that the UV spectra of such organic particulate UV filters in aqueous dispersion show certain shifts of the absorbance maximum and even occurrence of new bands, when compared to the UV spectra of the same molecules dissolved at micromolar concentrations in organic solvents [4–6]. This spectral broadening can be of advantage for the application in sunscreens, since today sunscreens are supposed to absorb in a broad spectral range, protecting the skin against UVB as well as UVA rays [7]. Bathochromic shifts in solid state UV–Vis spectra relative to the spectra in solution have been observed with organic pigments [8]. 1,3,5-triazine derivatives such as tris-biphenyl-triazine-type UV absorbers have been studied as host materials for organic light-emitting diodes [9]. In sunscreen applications, tris-biphenyl-triazine turned out to be a very photostable and efficient UV filter substance [10]. Photochemical and photo-physical deactivation of similar structures from 2,4,6-triaryl-1,3,5-triazines has been investigated in the past [11]. Recently, DFT calculations have been applied to study the excited-state molecular structures of butyl-methoxy-dibenzoyl-methane [12], and of benzotriazoles and different types of triazine UV absorbers, including tris-biphenyl-triazine [13].

In a previous paper, we have shown with quantum chemical calculations, that for a hydroxyphenyl-benzotriazole-type UV absorber in aqueous dispersion, the mentioned spectral effects can be explained by π-stacking of the chromophores in the particles [14]. In the present work, we investigated the origin of the spectral change, which occurs when TBPT is present in nanoparticles in aqueous dispersion, in comparison to being dissolved in an organic solvent, by means of DFT calculations. In

addition, we also used TD DFT calculations to study the electronic deactivation mechanism of this UV absorber. The insights may help being able to rationally design future materials for sunscreen applications.

2 Materials and methods

2.1 Experimental

The UV absorber investigated in this study is 2,4,6-tris(biphenyl-3-yl)-1,3,5-triazine, abbreviation TBPT, from BASF). The preparation of nano-particulate aqueous dispersions of the substance was performed with a ball-milling process [4] in deionized water using decyl glucoside (Plantacare 2000, BASF) as dispersant and xanthan gum (Rhodia) as thickener. 100 g of the aqueous dispersion contained 50 g of the UV absorber, 7.5 g decyl glucoside, 0.2 g xanthan gum, and 0.4 g propylene glycol (*Fluka*).

For UV–vis spectroscopic measurements in an organic solvent, stock solutions of defined concentrations of the UV absorber were prepared in dioxane (p.a., Fluka) and in ethanol (p.a., Merck), and diluted with the respective solvent. Aqueous dispersions were diluted with deionized water. UV–vis spectra of clearly dissolved UV absorbers were measured with a Perkin Elmer Lambda 650 UV/vis double-beam spectrometer in its standard setup. The sample solution and the reference (pure solvent) were filled into quartz cells of 1 cm optical path length and placed into the respective beams of the device. For measurements of the particulate absorbers, a Perkin Elmer Lambda Lambda 16 UV/vis double-beam spectrometer was employed with an integration sphere accessory in order to collect the direct transmitted light as well as the light scattered in forward direction. Sample and reference cells were placed in the respective light beams at their entrance into the integration sphere, while $BaSO_4$ pressings (Barium sulfate for white standard DIN 5033, Merck) were mounted into the sample and reference windows opposite thereof. Measurements were performed with a spectral resolution of 2 nm. In order to keep the samples as thin as possible, sandwich-type quartz cells with 0.0008 cm optical thickness (Hellma, Germany) were used for samples and reference. Since the reproducibility of experimental data with these cells was limited, for each individual suspension, 10 measurements with always freshly filled cells were averaged. The standard deviation was typically 7% of the average value.

Scanning Electron Microscopy (SEM) was performed using a Quanta 200 FEG device (FEI Company) with a high vacuum of 10^{-6} mbar, a high voltage of 10 kV and magnification of 50,000. The sample was sputtered with Au/Pd in order to achieve the necessary conductance.

2.2 Quantum chemical calculations

Density Functional Theory (DFT) calculations were carried out systematically employing the PBE0-D3 density functional [15–17]. The way in which the PBE0 functional is derived, and the lack of empirical parameters fitted to specific properties makes the PBE0 model a widely applicable method for quantum chemical calculations. The PBE0-D3 functional includes physically and chemically important London dispersion interactions [18]. The molecular geometries, energies, and electronic structure of the molecules were studied at PBE0-D3/6-31G** level of theory, as implemented in the Jaguar 9.6 program [19]. This computational model was already successfully used for calculations in our previous work [14, 20]. Frequency calculations were done at the same level of theory to obtain the total enthalpy (H) and Gibbs free energy (G) at a standard temperature of 298.15 K using unscaled frequencies. The reaction enthalpies (ΔH) and Gibbs free energies of reaction (ΔG) of studied molecules were calculated as the difference of the calculated H and G between the reactants and products, respectively. To take the solvent effect on the structure and reaction parameters of the studied molecules into account, the calculations were done using Jaguar's dielectric continuum Poisson–Boltzmann solver (PBF) [21], which fit the field produced by the solvent dielectric continuum ($\varepsilon = 2.2$ for dioxane, $\varepsilon = 24$ for ethanol and $\varepsilon = 80$ for water) to another set of point charges. The excited states and electronic transition spectra were calculated both in the gas phase and in the different solvents with the PBF solvation model using the Time-Dependent (TD) DFT method [22] at the PBE0-D3/6-31G** level of theory. The calculations for excited states were run with the Full Linear Response (FLR) approximation [23] as implemented in Jaguar 9.6 program. The number of excited states was set to 100 for two reasons: the first is that the initial guess might not accurately reflect the final states; the second is to ensure that near-degeneracies are accounted for. For the understanding of the mechanism of the photochemical deactivation of excited TBPT molecules, the geometry optimization of the first excited state was done with TD PBE0-D3/6-31G**/PBF for monomer in dioxane and for dimer and trimer in water. The Maestro 9.7 program [24] was used for the visualization of calculated UV–Vis spectra. The detailed procedure to obtain structures of different TBPT complexes multistep procedure is given in SI.

3 Results and discussion

3.1 Experimental data

Experimentally measured UV–Vis spectra of studied TBPT molecules both in dioxane and ethanol solution, as well as in aqueous dispersion are shown in Fig. 1A. Surprisingly, the observed UV–Vis spectra of TBPT molecules depend on experimental conditions. The UV–Vis spectra in aqueous dispersion differ from those in dioxane and ethanol not only by their position, but in their shape too. As shown in Fig. 1A, the absorption band of TBPT in dioxane lies in the UVB range with a λ_{max} at 314 nm and in ethanol at 315 nm. However, in aqueous dispersion, the UVB absorption band is broadened, and the maximum is slightly blue-shifted to 309 nm with a new shoulder arising at 338 nm. Figure 1B shows the SEM picture of TBPT particles from aqueous dispersion, demonstrating the existence of such particles in a size range of about 20–300 nm, consistent with a median size of 84 ± 13 nm based on a volume-weighted particle size distribution measured with fiber-optic quasi-elastic light scattering [25].

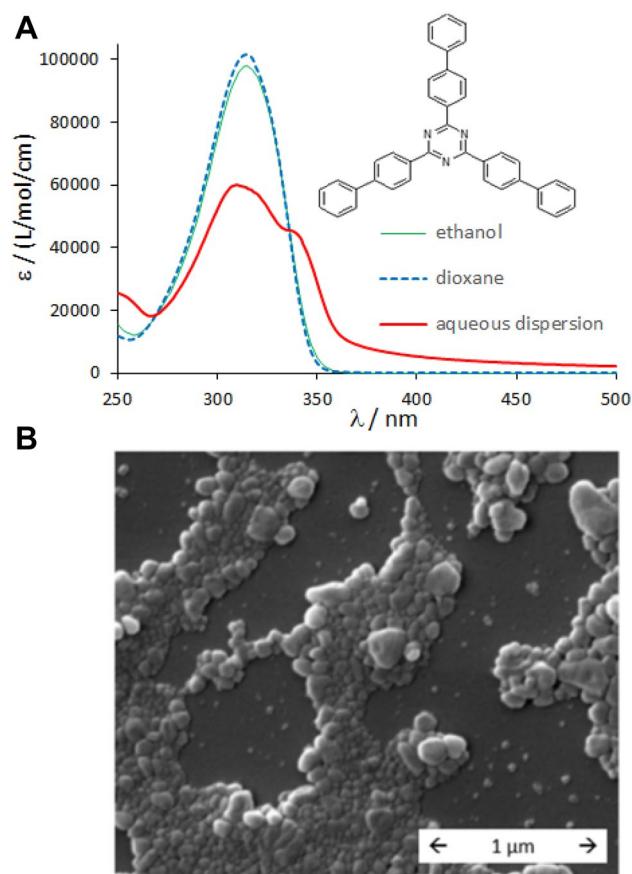

Fig. 1 A Experimental UV–Vis spectra of studied TBPT molecules in ethanol and dioxane solutions and in aqueous dispersion. B SEM image of particulate TBPT UV absorbers from aqueous dispersion

3.2 UV/vis spectra of TBPT from quantum chemical calculations.

In order to better understand the different spectra of TBPT in organic solvents and in particles, we carried out quantum chemical calculations. The structures, electron distributions of molecular orbitals involved into formation of UV/Vis spectra, and energetics of possible dimer formations of studied molecules were investigated. Additionally, the mechanism of photochemical deactivation of the photochemically excited TBPT molecules was studied in detail.

The molecular structure of TBPT is depicted in Fig. 1A and the most stable optimized structure of TBPT is shown in Fig. 2A. The electron distributions from molecular orbitals (MO) mostly involved in the formation of low energy excited states are shown in Fig. 2B.

To get more information about origin, structure and effect of solvent on experimental UV–Vis spectra of studied TBPT molecules calculations were done on the monomer TBPT in different solvents. The results of calculations are shown in Fig. 3 and excitation energies are given in Table 1. The calculated UV–Vis spectra in dioxane ethanol and water have strong absorption bands with maxima at 312 nm, 316 nm, and 324 nm, respectively. As can be seen, there is only a small effect of solvent as dielectric continuum (within 10 nm relative to gas phase) on the calculated UV–Vis spectra of isolated molecule. It may be apparently caused by low solvation energy ($Esolv = 36$ kJ mol^{-1} in water) of TBPT molecule. The calculated UV–Vis spectra in dioxane and ethanol are in
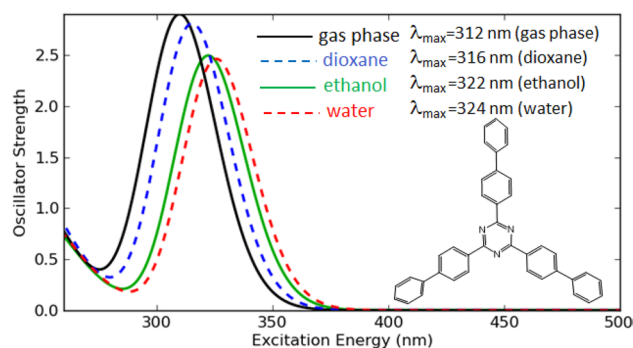

Fig. 3 UV–Vis spectra of the TBPT monomer calculated at optimized in corresponding solvent molecular structure with TD PBE0-D3/6-31G**/PBF in dependence on solvent

very good agreement with experimental ones observed at 314 and 315 nm, respectively.

However, the UV–Vis spectrum of TBPT observed in aqueous dispersion (Fig. 1A) with a maximum at 309 nm and a shoulder at 338 nm differs strongly from the one calculated in water with a maximum at 324 nm. This cannot be explained with the absorption of isolated TBPT molecules. It was supposed, that due to the low solubility of TBPT in water, different aggregates could be formed, such as dimer, trimer, or higher π-stacked complexes, which may be responsible for the observed structure of UV–Vis spectra in aqueous dispersion. First, the possibility of building dimeric structures of TBPT in water was studied. Two stable and energetically favorable dimeric complexes of TBPT were found (shown in Fig. 4) with complex (A) being by 50 kJ mol^{-1} more stable than complex (B). As

Fig. 2 Most stable optimized structure of TBPT (**A** front view and side view); **B** electron distributions from molecular orbitals (MOs) mostly involved in the formations of low energy excited states
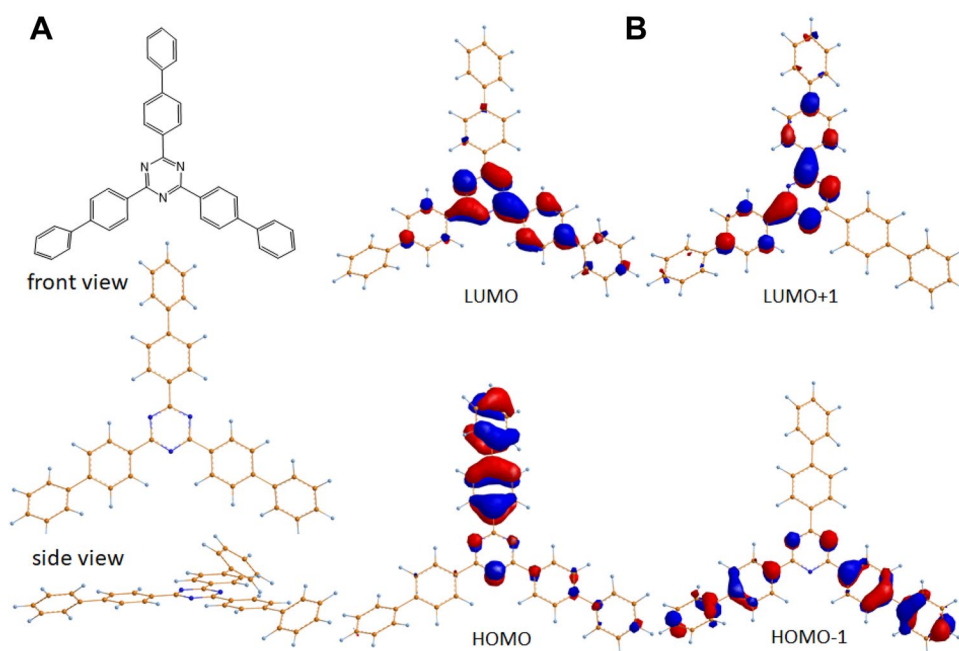
Table 1 Experimental results in dioxane, ethanol solution and aqueous dispersion in comparison with calculated results UV–Vis (λ in nm) of TBPT

	λ_{max} (exp)	λ_{max} (calc)	Λ (S^n) (calc)	f	Transition
Gas phase monomer			320	0.0002	$S^0 -> S^1$
		312	316	1.2683	$S^0 -> S^2$
Dioxane monomer			324	0.0003	$S^0 -> S^1$
	314	316	320	1.2390	$S^0 -> S^2$
Ethanol monomer			325	0.0007	$S^0 -> S^1$
	315	322	323	1.2450	$S^0 -> S^2$
Water monomer			329	0.0014	$S^0 -> S^1$
		324	326	1.2290	$S^0 -> S^2$
Water dimer			336	0.0075	$S^0 -> S^1$
	338		334	0.0634	$S^0 -> S^2$
			326	0.0578	$S^0 -> S^5$
	309	314	324	0.4358	$S^0 -> S^6$
Complex 3 units			340[b]	0.0226	$S^0 -> S^1$
	338	325[a]	336	0.0435	$S^0 -> S^2$
			331	0.0687	$S^0 -> S^3$
	309	308	321	0.2446	$S^0 -> S^{12}$
			319	0.7365	$S^0 -> S^{14}$
Complex 4 units			350[b]	0.0124	$S^0 -> S^1$
	338	322[a]	340	0.0350	$S^0 -> S^2$
			331	0.0466	$S^0 -> S^5$
	309	306	325	0.2355	$S^0 -> S^{10}$
			320	0.4261	$S^0 -> S^{17}$
			310	0.3555	$S^0 -> S^{29}$
Complex 5 units			351[b]	0.0107	$S^0 -> S^1$
	338	323[a]	340	0.0264	$S^0 -> S^2$
			327	0.0825	$S^0 -> S^7$
			325	0.1651	$S^0 -> S^{10}$
	309	305	312	0.2211	$S^0 -> S^{29}$
			307	0.4356	$S^0 -> S^{40}$
			305	0.3888	$S^0 -> S^{47}$

Here λ_{max} is the maximum of the low energy absorption band and $\lambda(S^n)$ is the energy of the S^n excited state calculated in gas phase, dioxane, ethanol and water, f is the oscillator strength

[a] λ_{max} (calc) according to UV–Vis spectra given in Fig. 6

[b] Selected most intensive transitions responsible for the line shape of the calculated UV–Vis. Additionally, the calculated absorption spectrum data for the TBPT complexes with 4- and 5 units are given in SI

calculated, the formation of the TBPT dimer is energetically favorable both in gas phase and in water. For the most stable TBPT dimer (A), the calculated reaction enthalpy ΔH and Gibbs free energy ΔG of dimer formation in the gas phase are -126 kJ mol^{-1} and -38 kJ mol^{-1}, respectively. The formation of the TBPT dimer (A) in water is exergonic too, with ΔH and ΔG of dimer formation -119 kJ mol^{-1} and -36 kJ mol^{-1}, respectively. The most stable TBPT-dimers (A) and (B) (shown in Fig. 4) are stabilized through interaction between π-electrons localized on rings from two parts of the dimer. The smallest distances between the two parts of the optimized dimer (A) are 0.354 nm in gas phase and 0.346 nm in water.

Moreover, different energetically favorable stable complexes of TBPT up to 5 molecules were optimized with mean stabilization electronic energy per unit 113 kJ mol^{-1}. The most stable optimized in gas phase structures of complexes with three, four and five molecules are shown in Fig. 5. The parallel structure (sandwich geometry) of the most favorable dimer and oligomers indicate the H-type of complex. Additionally, the Cartesian coordinates of geometry optimized structures of TBPT monomers and difference stable complexes are given in Supporting Information.

The calculations of UV–Vis spectra of TBPT complexes with three, four and five molecules were done on structure optimized in the gas phase, because of the small effect of
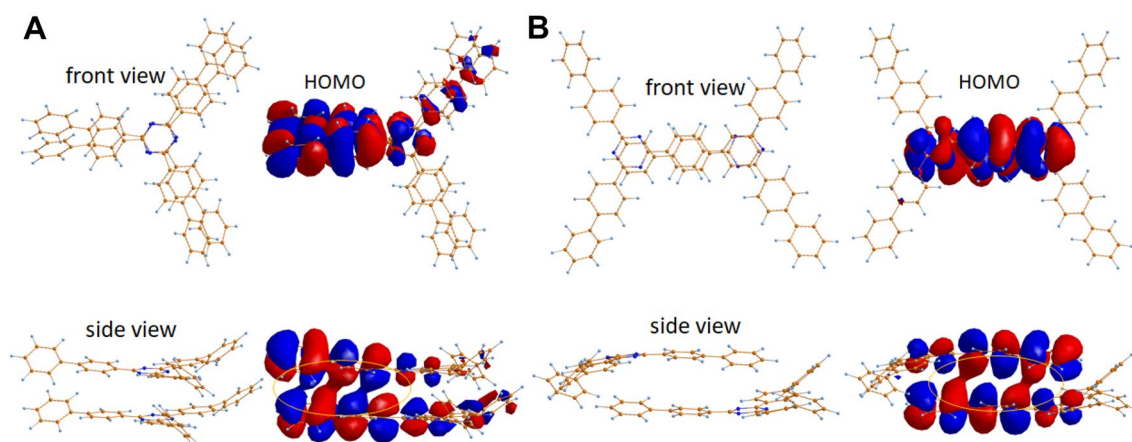
Fig. 4 Calculated in water two most stable structures and HOMO of MBBT dimers: dimer (**A**) is 50 kJ mol^{-1} energetically more favorable than dimer (**B**)
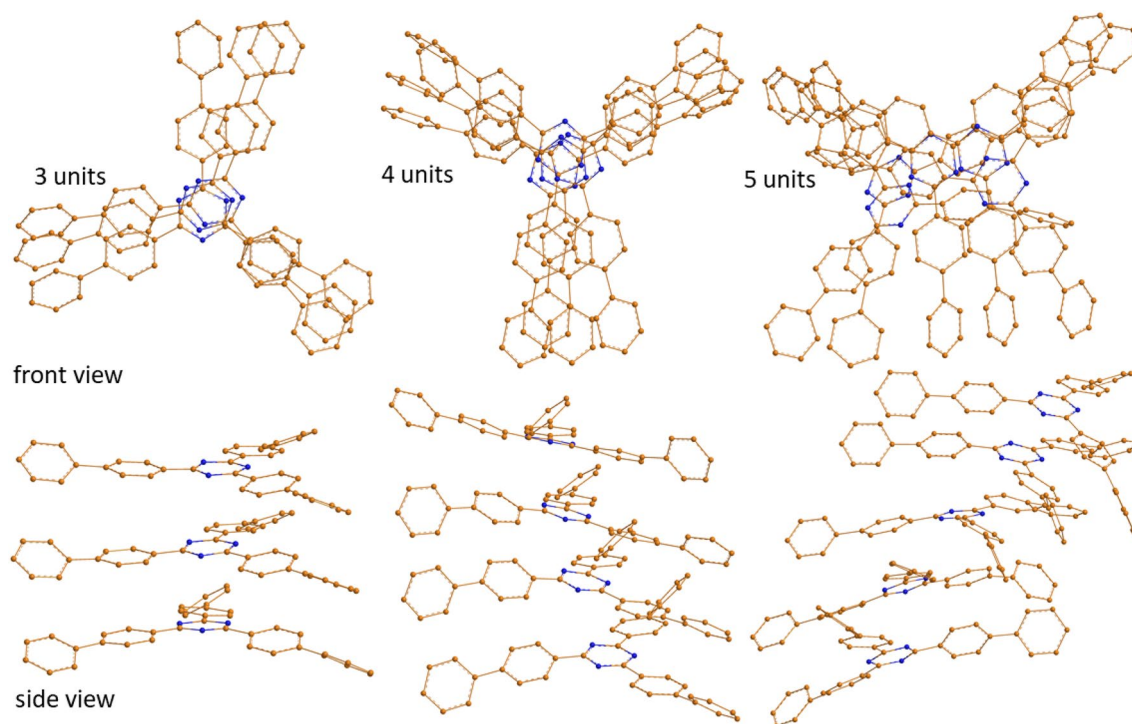

Fig. 5 Optimized most stable structures of π-stacked complexes of TBPT molecules. H-atoms are omitted

water as dielectric continuum in this case. The changes of calculated in gas phase UV/vis spectra of isolated TBPT molecules and different energetically favorable stable complexes in dependence on the number of TBPT up to 5 molecules are shown in Fig. 6.

As can be seen, the shape of calculated UV–Vis spectra of TBPT complexes differs from those for isolated TBPT monomer. The absorption maximum is systematically blue-shifted to 305 nm in dependence on the number of

molecules in complex, and the shoulder grows at 325 nm. As can be seen, the shape and position of UV–Vis spectra of TBPT complexes is in better agreement with those observed in aqueous dispersion. Thus, the possibility of the building of oligomeric structures of TBPT in water may be the reason of the experimentally observed difference between the UV–Vis spectra in dioxane and aqueous dispersion.
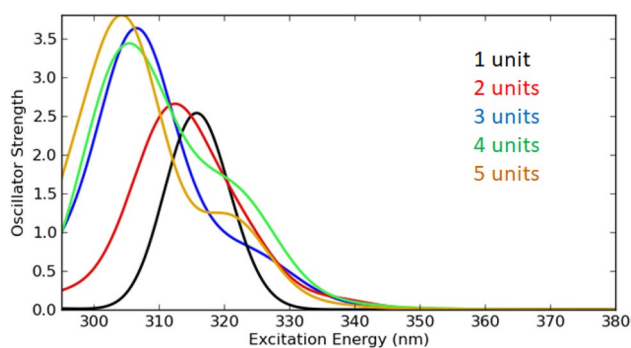
Fig. 6 Calculated in gas phase UV–Vis spectra of TBPT complexes up to 5 molecules

3.3 Mechanism of deactivation of excited TBPT

DFT calculations were done to get more information on the possible mechanism of deactivation of the TBPT molecule after excitation. The calculated excitation energy scheme (Jablonski diagram) for the case of an isolated TBPT molecule in dioxane is shown in Fig. 7a. The excitation should be mostly into $*S^2$ excited singlet state, which has very strong oscillator strength, followed by structural relaxation into the

S^1 excited state. Further, by intersystem crossing (ISC), the triplet state $*T^1$ will be populated, which undergoes further relaxation through adjustment of the molecular geometry to the changes of the electron distributions induced by the excitation. The relaxed T^1 excited state could be deactivated either through phosphorescence or vibrational relaxation. However, due to the low energy of T^1 (2.7 eV), deactivation should go preferably radiationless through vibrational relaxation. Additionally, the possible decomposition of the isolated TBPT molecule into reactive radicals from T^1 was calculated to be strong endergonic ($\Delta G = 45$ kcal mol^{-1}), apparently due to formation of energetically unfavorable phenyl type of radicals. That is in agreement with the strong stability of TBPT.

To study the effect of water, where the formation of TBPT complexes was observed, the corresponding calculations were done on the TBPT dimer and trimer in water (shown in Fig. 7b and c). In the case of the TBPT dimer in water (Fig. 7b), the excitation should be into $*S^2$ and higher energy excited singlet states, which has very strong oscillator strength. After structural relaxation, the optimized S^1 excited state will build up which has much lower energy in comparison with the TBPT monomer in dioxane. After intersystem crossing (ISC), the triplet state $*T^1$ will be populated,
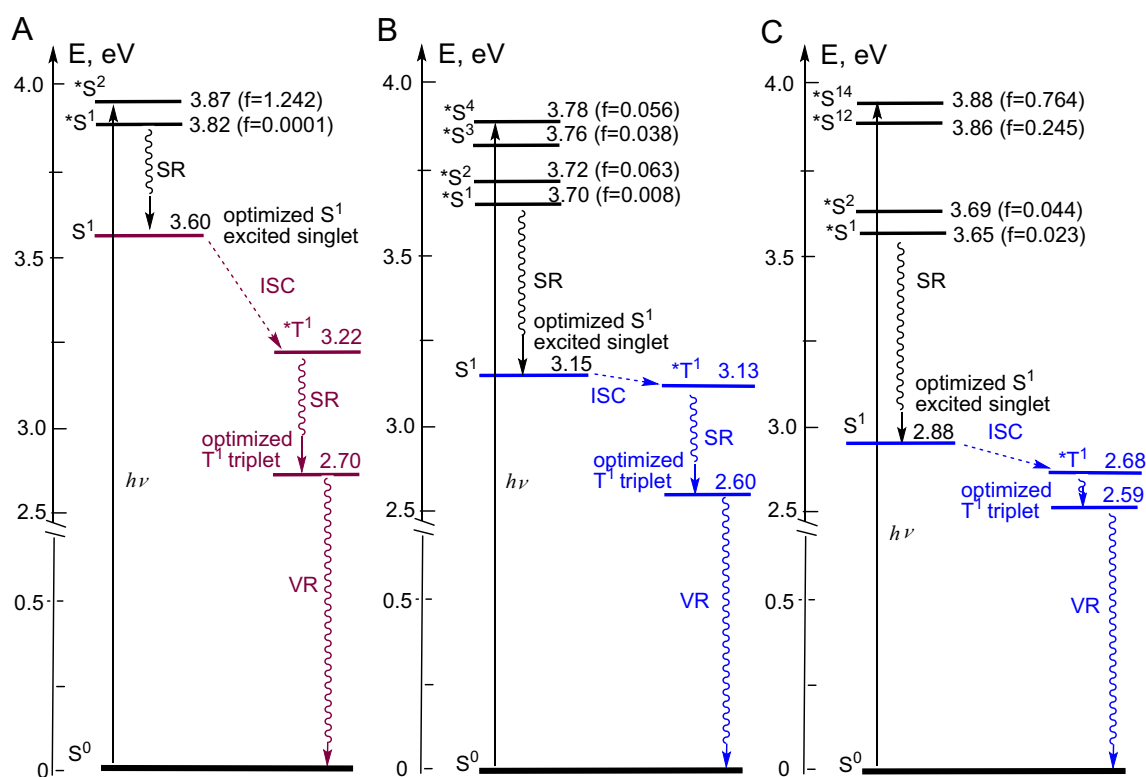

Fig. 7 Calculated excitation energy scheme (Jablonski diagram) of TBPT: **a** TBPT isolated molecule in dioxane; **b** TBPT dimer in water (S^1 excited state was optimized with TD PBE0-D3/6-31G**/PBF method); **c** TBPT trimer in water. Here SR denotes structural relaxation during optimization of first exited state, and VR denotes vibrational relaxation

which undergoes further relaxation through adjustment of the molecular geometry to the changes of the electron distributions induced by the excitation. Again, the energy of both $*T^1$ and relaxed T^1 excited states is lower than those of the TBPT monomer in dioxane. The trends of further energy lowering of relaxed S^1 and T^1 excited states were calculated for the case of TBPT trimers in water (Fig. 7c). As follows, the low energy of T^1 excited state will support radiationless energy deactivation through vibrational relaxation. It should be noted, that radiationless energy deactivation in aqueous dispersion will be strongly supported by high energy OH vibrations of water molecules. Unfortunately, all attempts to analyze TBPT oligomers with 4 and 5 units were unsuccessful, the complexes were not stable during optimization in excited state.

Nevertheless, based on the existing data, we can assume that there is a decrease of the triplet energy with increasing size of the aggregates. This is of practical interest, as the TBPT particles shown in Fig. 1B have an average size of about 60 nm. With a density of the material of 1.12 g/cm^3, the "molecular weight" of one such particle is $7.6 \cdot 10^7$ g/mol, corresponding to $1.4 \cdot 10^5$ TBPT molecules per particle. We may thus regard the particles as huge aggregates with presumably low T^1 energy of the TBPT molecules making up the particles. For this reason, it is unlikely that the material will act as a triplet sensitizer for acceptor molecules.

4 Summary and conclusions

Experimental UV/Vis spectra of TBPT in solution in dioxane and ethanol, as well as in aqueous dispersion were compared with calculated UV–Vis spectra (DFT) in different solvents of the respective monomers, dimers, and aggregates. The following conclusions may be drawn on the basis of the quantum chemical analysis. The calculated UV–Vis spectra of isolated TBPT molecules in dioxane and ethanol agree well with experimentally observed ones. The solvent effect of water as dielectric continuum is small and cannot explain the observed changes in the shape and position of UV–Vis spectra in aqueous dispersion. Apparently, due to low solubility in water, TBPT molecules could build stable energetically favorable complexes. The calculated UV–Vis spectra of different π-stacked complexes of TBPT molecules are in reasonable agreement in shape and position with experimentally observed UV–Vis spectra in aqueous dispersion. With TBPT particles in aqueous dispersion, the absorption maximum at 315 nm in ethanol is shifted to 309 nm, and an additional absorption band occurs at 338 nm, the latter one only observed with the aqueous dispersion of TBPT particles. A similar behavior is obtained in the calculated results, where the low-wavelength absorption maximum calculated for the TBPT aggregates as well is shifted hypsochromically to

305 nm, while a second absorption band develops at 320 nm with increasing aggregate size. Although the wavelength of this additional band is smaller than the experimentally observed one at 338 nm, the calculations are qualitatively in agreement with the experimental observations. A reason for the deviation of the wavelength at which the bathochromically observed band occurs, may be the difference in aggregate size looked at in the experiment and the calculations. For a TBPT particle of 84 nm diameter and a density of 1.256 g/cm^3 [25], one can estimate an aggregation number of about $4 \cdot 10^5$, where in the calculations we employed aggregate sizes up to five.

TBPT shows a low lying T^1 state which is further decreased in the aggregates, supporting radiationless energy dissipation and decreasing the probability of triplet sensitization of acceptor molecules.

It is not possible to anticipate the UV spectra of organic particulate UV absorbers in aqueous dispersion from UV spectra of the isolated absorber molecules in organic solvents. However, it has been shown in this work that application of quantum chemical calculations can contribute to the understanding of UV spectra of organic particulate UV absorbers and may be used to predict the behavior of similar systems in future.

Data Availability Data are available upon request from the authors.

Declarations

Conflict of interest The authors declare that they do not see any conflict of interest.

References

1. Hanay, C., & Osterwalder, U. (2021). *Current problems in dermatology* (55th ed., pp. 93–111). Karger.

2. Olmo, M. D., Navarro, A., Garcia, C., Hear, T., & Beltran, L. (2022). Effects of structure on the solubility of UV filters. *Cosmetics, 9*, 60–65.

3. Herzog, B., Katzenstein, A., Quass, K., Stehlin, A., & Luther, H. (2004). Physical properties of organic particulate UV absorbers used in sunscreens. I. Determination of particle size with fiber-optic quasi-elastic light scattering (FOQELS), disc centrifugation, and laser diffractometry. *Journal of Colloid and Interface Science, 271*, 136–144.

4. Mueller, S., Herzog, B., Giesinger, J., Quass, K., & Osterwalder, U. (2005). Micronization as a tool in the development of innovative UV filters. *SOFW Journal, 131*, 32–38.

5. Herzog, B., Quass, K., Schmidt, E., Mueller, S., & Luther, H. (2004). Physical properties of organic particulate UV absorbers used in sunscreens. II. UV-attenuating efficiency as function of particle size. *Journal of Colloid and Interface Science, 276*, 354–363.

6. Hüglin, D. (2016). Advanced UV absorbers for the protection of human skin. *Chimia, 70*, 496–501.

7. Hughes, S. N. G., Lowe, N. J., Gross, K., Mark, L., Goffe, B., Hughes, H., & Cole, C. (2021). *Current problems in dermatology* (55th ed., pp. 157–169). Karger.

8. Mizuguchi, J., & Rihs, G. (1992). Electronic spectra of 1,4-Diketo-3,6-Diphenyl-Pyrrolo-[3,4-c]-Pyrrole in the solid state. *Berichte der Bunsengesellschaft Physical Chemistry, 96*, 597–606.

9. Chen, H.-F., Yang, S.-J., Tsai, Z.-H., Hung, W.-Y., Wang, T.-C., & Wong, K.-T. (2009). 1, 3, 5-Triazine derivatives as new electron transport–type host materials for highly efficient green phosphorescent OLEDs. *Journal of Materials Chemistry, 19*, 8112–8118.

10. Couteau, C., Paparis, E., Chauvet, C., & Coiffard, L. (2015). Tris-biphenyl triazine, a new ultraviolet filter studied in terms of photoprotective efficacy. *International Journal of Pharmaceutics, 487*, 120–123.

11. Elbe, F., Keck, J., Fluegge, A. P., Kramer, H. E. A., Fischer, P., Hayoz, P., Leppard, D., Rytz, G., Kaim, W., & Ketterle, M. (2000). Photochemical and photophysical deactivation of 2,4,6-triaryl-1,3,5-triazines. *Journal of Physical Chemistry A, 104*, 8296–8306.

12. Pinto da Silva, L., Ferreira, P. J. O., Duarte, D. J. R., Miranda, M. S., & Esteves da Silva, J. C. G. (2014). Structural, energetic, and UV–Vis spectral analysis of UVA filter 4-tert-butyl-4′-methoxydibenzoylmethane. *Journal of Physical Chemistry A, 118*, 1511–1518.

13. Santos, B. A. M. C., da Silva, A. C. P., Bello, M. L., Gonçalves, A. S., Gouvêa, T. A., Rodrigues, R. F., Cabral, L. M., & Rodrigues, C. R. (2018). Molecular modeling for the investigation of UV absorbers for sunscreens: Triazine and benzotriazole derivatives. *Journal of Photochemistry and Photobiology A, 356*, 219–229.

14. Naumov, S., Herzog, B., & Abel, B. (2020). Spectra and photorelaxation of hydroxyphenyl-benzotriazole-type UV absorbers: From monomers to nanoparticles. *Journal of Physical Chemistry A, 124*, 625–632.

15. Perdew, J. P., Burke, K., & Ernzerhof, M. (1996). Generalized gradient approximation made simple. *Physical Review Letters, 77*(18), 3865–3868.

16. Perdew, J. P., Burke, K., & Ernzerhof, M. (1997). Generalized gradient approximation made simple. *Physical Review Letters, 78*(7), 1396.

17. Adamo, C., & Barone, V. (1999). Toward reliable density functional methods without adjustable parameters: The PBE0 model. *The Journal of Chemical Physics, 110*(13), 6158–6169.

18. Grimme, S., Antony, J., Ehrlich, S., & Krieg, H. (2010). A consistent and accurate ab initio parametrization of density functional dispersion correction (DFT-D) for the 94 elements H-Pu. *The Journal of Chemical Physics, 132*(154104), 1–19.

19. Jaguar, version 9.6. (2017). Schrodinger, Inc., New York, NY

20. Weilbeer, C., Sickert, M., Naumov, S., & Schneider, C. (2017). The Brønsted acid-catalyzed, enantioselective Aza-Diels-Alder reaction for the direct synthesis of chiral piperidones. *Chemistry A European Journal, 23*, 513–518.

21. Tannor, D. J., Marten, B., Murphy, R., Friesner, R. A., Sitkoff, D., Nicholls, A., Ringnalda, M., Goddard, W. A., III., & Honig, B. (1994). Accurate first principles calculation of molecular charge distributions and solvation energies from Ab initio quantum mechanics and continuum dielectric theory. *Journal of the American Chemical Society, 116*, 11875–11882.

22. Bauernschmitt, R., & Ahlrichs, R. (1996). Treatment of electronic excitations within the adiabatic approximation of time dependent density functional theory. *Chemical Physics Letters, 256*, 454–464.

23. Pollard, W., & Friesner, R. A. (1993). Efficient Fock matrix diagonalization by a Krylov-space method. *The Journal of Chemical Physics, 99*, 6742–6750.

24. Schrödinger Release 2017–2. (2017). Maestro, Schrödinger, LLC, New York

25. https://ec.europa.eu/health/scientific_committees/consumer_safety/docs/sccs_o_070.pdf. Accessed 3 Mar 2022

Authors and Affiliations

Sergej Naumov[1] · Bernd Herzog[2] · Bernd Abel[1,3]

✉ Bernd Abel
bernd.abel@uni-leipzig.de

1　Leibniz Institute of Surface Engineering (IOM), Permoserstrasse 15, 04318 Leipzig, Germany

2　BASF Grenzach GmbH, Koechlinstr. 1, 79639 Grenzach-Wyhlen, Germany

3　Institute of Chemical Technology and Wilhelm-Ostwald-Institute of Physical and Theoretical Chemistry, Linnestrasse 3, 04103 Leipzig, Germany